



## Precursory Behavior of Groundwater Radon in Southeastern Taiwan: Effect of Tectonic Setting in the Subduction Zone

T. KUO,<sup>1,2</sup> W. CHEN,<sup>3</sup> C. LEWIS,<sup>1</sup> C. HO,<sup>4,5</sup> and H. KUOCHEN<sup>4</sup>

**Abstract**—Monitoring precursory decline in groundwater radon at the Antung hot spring is a useful means of forecasting the magnitude and precursor time of local disastrous earthquakes. With the help of a case study in southeastern Taiwan, this paper demonstrates the effect of tectonic setting in the subduction zone on the correlation between radon decline, precursory time and earthquake magnitude. Given a radon-monitoring site located near the plate boundary in the tectonic setting of advanced arc-continental collision, the observed radon decline and precursory time prior to the earthquakes in the tectonic setting of initial arc-continental collision are smaller than those observed prior to the earthquakes occurring on the plate boundary in the tectonic setting of advanced arc-continental collision. In the advanced arc-continental collision state, the coupling between the plates is strong and the stress transfer is efficient, whereas in the incipient collision state, the coupling and stress transfer are not as good. It also takes additional time lag and attenuation for the stress transfer from one tectonic setting to the other. This paper presents the difference in the precursory behavior of groundwater radon between earthquakes which occurred in two different tectonic settings: advanced and initial arc-continental collision.

**Keywords:** Radon, groundwater, earthquakes, tectonic setting, subduction.

### 1. Introduction

Variations of radon concentration (Radon-222) in groundwater have been applied as possible precursor in earthquake prediction studies (Noguchi and Wakita

1977; Wakita et al. 1980; Shapiro et al. 1980; Hauksson 1981; Igarashi et al. 1995; Papastefanou 2002; Baykara and Dođru, 2006; Kuo et al. 2006a; Zmazeka et al. 2006; Erees et al. 2007; Yalim et al. 2007; Namvaran and Negarestani 2013; Tarakçi et al. 2014; Skelton et al. 2014; Nevinsky et al. 2015). Radon anomalies measured in groundwater prior to earthquakes often showed increases in radon concentration (Hauksson 1981). A few radon anomalies exhibited decreases in radon concentration (Wakita et al. 1980; Shapiro et al. 1980; Kuo et al. 2006a). We have focused on anomalous declines in groundwater radon in southeastern Taiwan since 2003.

Anomalous decreases in radon concentration were observed in groundwater prior to the Taiwan 2003 Chengkung earthquake of magnitude  $M_w$  6.8 (Kuo et al. 2006a). The 2003  $M_w$  6.8 Chengkung was the strongest earthquake near the Chengkung area in eastern Taiwan since 1951. Mechanisms and geological conditions for interpreting anomalous decreases in radon prior to earthquakes are seldom discussed in the literature. The Antung hot spring is a low-porosity fractured small aquifer situated in an andesitic block and surrounded by a ductile mudstone of the Lichi mélange (Chen and Wang 1996). Regarding a physical basis that explains the anomalous decrease in radon concentration in groundwater prior to the 2003 Chengkung earthquake, a mechanism of radon volatilization was presented based on radon phase behavior and the geological conditions of the Antung hot spring (Kuo et al. 2006b).

We initiated an observation of groundwater radon in July 2003 at well D1 located at the Antung hot spring (Fig. 1). Well D1 is 3 km southeast of the Chihshang fault (Longitudinal Valley fault). The fault ruptured during two 1951 earthquakes of magnitudes

<sup>1</sup> Department of Mineral and Petroleum Engineering, National Cheng Kung University, Tainan, Taiwan. E-mail: mctkuobe@mail.ncku.edu.tw

<sup>2</sup> NCKU Research and Development Foundation, Tainan, Taiwan.

<sup>3</sup> Department of Geosciences, National Taiwan University, Taipei, Taiwan.

<sup>4</sup> Institute of Geophysics, National Central University, Zhongli, Taiwan.

<sup>5</sup> Central Weather Bureau, Taipei, Taiwan.

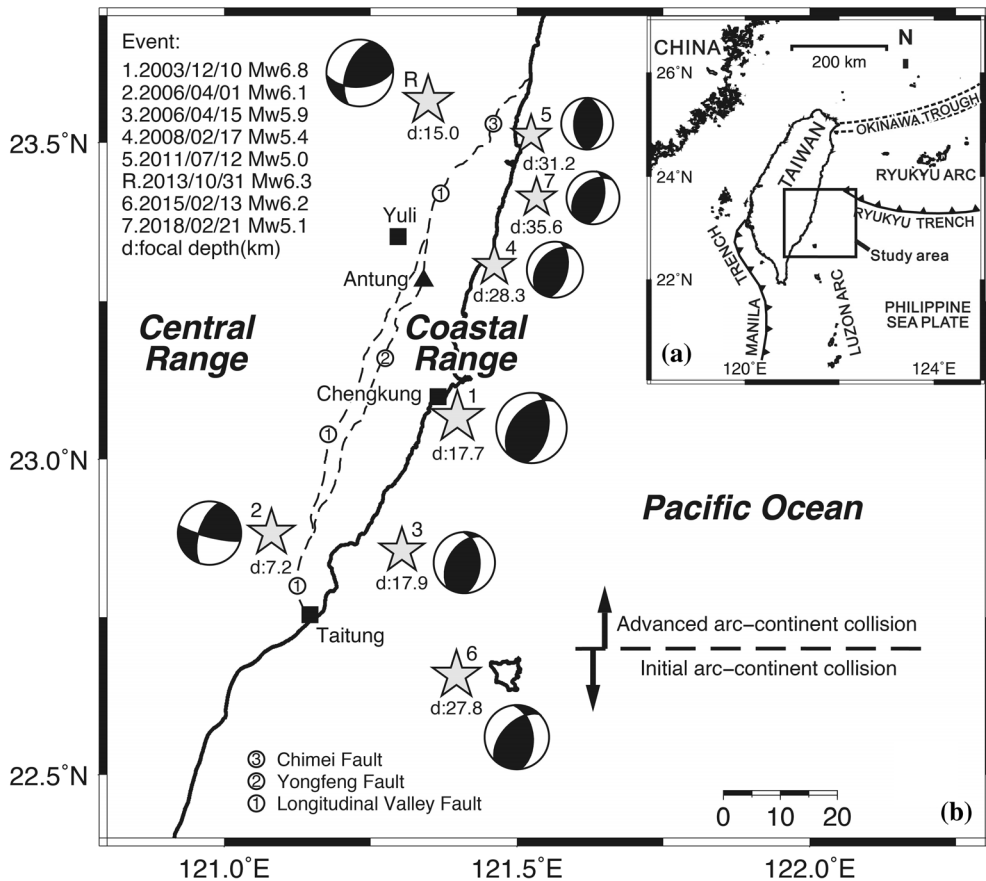


Figure 1

Map of the epicenters of the large earthquakes that occurred near Antung from 2003 to 2018. **a** Map of Taiwan. **b** Study area near the Antung hot spring (filled stars: mainshocks, filled triangle: radon-monitoring well D1)

M 6.2 and M 7.0 (Hsu 1962). The Longitudinal Valley fault is part of the boundary of the present-day plate suture between the Eurasia and the Philippine Sea plates. Since July 2003, recurrent radon anomalies were observed at well D1 to precede the following seven large earthquakes: the Chengkung  $M_w$  6.8 (December 10, 2003); Taitung  $M_w$  6.1 (April 1, 2006) and  $M_w$  5.9 (April 15, 2006); Antung  $M_w$  5.4 (February 17, 2008); Chimei  $M_w$  5.0 (July 12, 2011); Green Island  $M_w$  6.2 (February 13, 2015); and Changbin  $M_w$  5.1 (February 21, 2018) quake. We consider the 2006  $M_w$  5.9 Taitung earthquake that occurred on April 15th to have been triggered by stress transfer in response to the 2006  $M_w$  6.1 Taitung earthquake.

Well D1 is located 24 km, 52 km, 47 km, 13 km, 32 km, 69 km, and 25 km, respectively, from the epicenters of seven events, i.e., the 2003 Chengkung  $M_w$  6.8, 2006 Taitung  $M_w$  6.1 and  $M_w$  5.9, 2008 Antung  $M_w$  5.4, 2011 Chimei  $M_w$  5.0, 2015 Green Island  $M_w$  6.2, and 2018 Changbin  $M_w$  5.1 earthquakes (Fig. 1). The above earthquakes occurred in two different tectonic settings of southeastern Taiwan. Well D1 and the epicenters of Event 1, 2, 3, 4, 5, and 7 [the 2003 Chengkung, 2006 Taitung (two quakes), 2008 Antung, 2011 Chimei, and 2018 Changbin earthquakes] are located near the plate boundary (the Longitudinal Valley Fault), representing an advanced arc-continent collision stage of tectonic development. Epicenters of Event 1, 3, 4, 5, and 7 lie in the ocean on the Philippine Plate, whereas

the Event 2 epicenter (Fig. 1) lies on the Eurasia Plate. The epicenter of offshore Event 6 (the 2015 Green Island earthquake) was located on the Luzon volcanic arc that is undergoing initial arc-continent collision (Fig. 1). This arc extends from eastern Taiwan to the Philippines. Huang et al. (2006) presented a tectonic map showing active arc-continent collision in Taiwan. As shown in Fig. 1, the boundary between the initial arc-continent collision and advanced arc-continent collision zones is currently about latitude  $22.7^{\circ}$  N. Chen (2009) illustrated the tectonic framework of southeastern Taiwan offshore using a block diagram. Figure 2a shows the tectonic setting near Green Island currently in the stage of initial arc-continent collision (about latitude  $21.0\text{--}22.7^{\circ}$  N). Figure 2b shows the tectonic setting near Coastal Range currently in the stage of advanced arc-continent collision (about latitude  $22.7\text{--}23.5^{\circ}$  N).

Well D1 and the epicenters of Event 1, 3, 4, 5, and 7 are all located near the plate boundary in the Coastal Range, which represents an advanced arc-continent collision. With the radon anomalous decline observed prior to the 2015  $M_w$  6.2 Green Island earthquake (Event 6), we now have the opportunity to compare the precursory behavior of groundwater radon for the advanced and initial arc-continent collision stages. The objectives of this paper are to: (1) present the radon anomalous decline observed at Well D1 prior to the 2015  $M_w$  6.2 Green Island incipient collision zone earthquake, and (2) investigate the effect of tectonic setting on the correlation between radon decline, precursory time and earthquake magnitude in southeastern Taiwan.

## 2. Materials and Methods

### 2.1. Geological Setting

The Antung area is in a unique tectonic setting located at the boundary between the Eurasian and Philippine Sea plates. Figure 3 shows the geological map and cross section near the radon-monitoring well D1 in the Antung area. The Antung hot spring is situated in an andesitic tuffaceous sandstone block (Miocene) which is enclosed within the Paliwan Formation (Late Pliocene to Pleistocene) of

alternating thin-bedded sandstone and shale. The hot spring is formed nearby an eastward-dipping, high-angle reverse fault zone which contacts between the Lichi mélangé and the Paliwan Formation. Some hot springs and mud volcanoes are scattered along the fault zone, indicating a Quaternary active fault. Four stratigraphic units are present (Chen and Wang 1996). The Tuluanshan Formation consists of Miocene volcanic units such as lava and volcanic breccia as well as tuffaceous sandstone. The Fanshuliao (Pliocene) and Paliwan (Late Pliocene to Pleistocene) Formations consist of rhythmic sandstone and mudstone turbidites. The Lichi mélangé occurs as a highly deformed mudstone that is characterized by penetrative foliation visible in outcrop.

Well-developed minor faults and joints are common in the tuffaceous-sandstone block displaying intensively brittle deformation. It is possible that these fractures reflect deformation and disruption by the nearby faults. Ground water flows through the fault zone and is then diffused into the block along the minor fractures. The radon-monitoring well D1 is not artesian, implying a weak recharge to a small aquifer in un-drained conditions. Hence, geological evidence suggests that the Antung hot spring at well D1 is a small low-porosity fractured aquifer in un-drained conditions near an active fault.

Under such geological conditions as the Antung hot spring, two physical processes, rock dilatancy and water diffusion, are likely to take place. When the regional stress increases to about half the fracture stress, rock dilatancy initiates and cracks develop in aquifer rock (Brace et al. 1966). According to the dilatancy-diffusion model (Nur 1972; Scholz et al. 1973), the development of new cracks in the aquifer rock could occur at a rate faster than the recharge of pore water. In a small aquifer with un-drained conditions, gas saturation could develop in the rock cracks. When gas phase develops in aquifer rock, the radon in groundwater volatilizes into the gas phase and the radon concentration in groundwater decreases. The above mechanism is also referred to as “in situ radon volatilization” (Kuo et al. 2006b).

A small low-porosity fractured aquifer near an active fault (e.g., the Antung hot spring) is a suitable geological site to detect precursory declines in groundwater radon prior to local large earthquakes

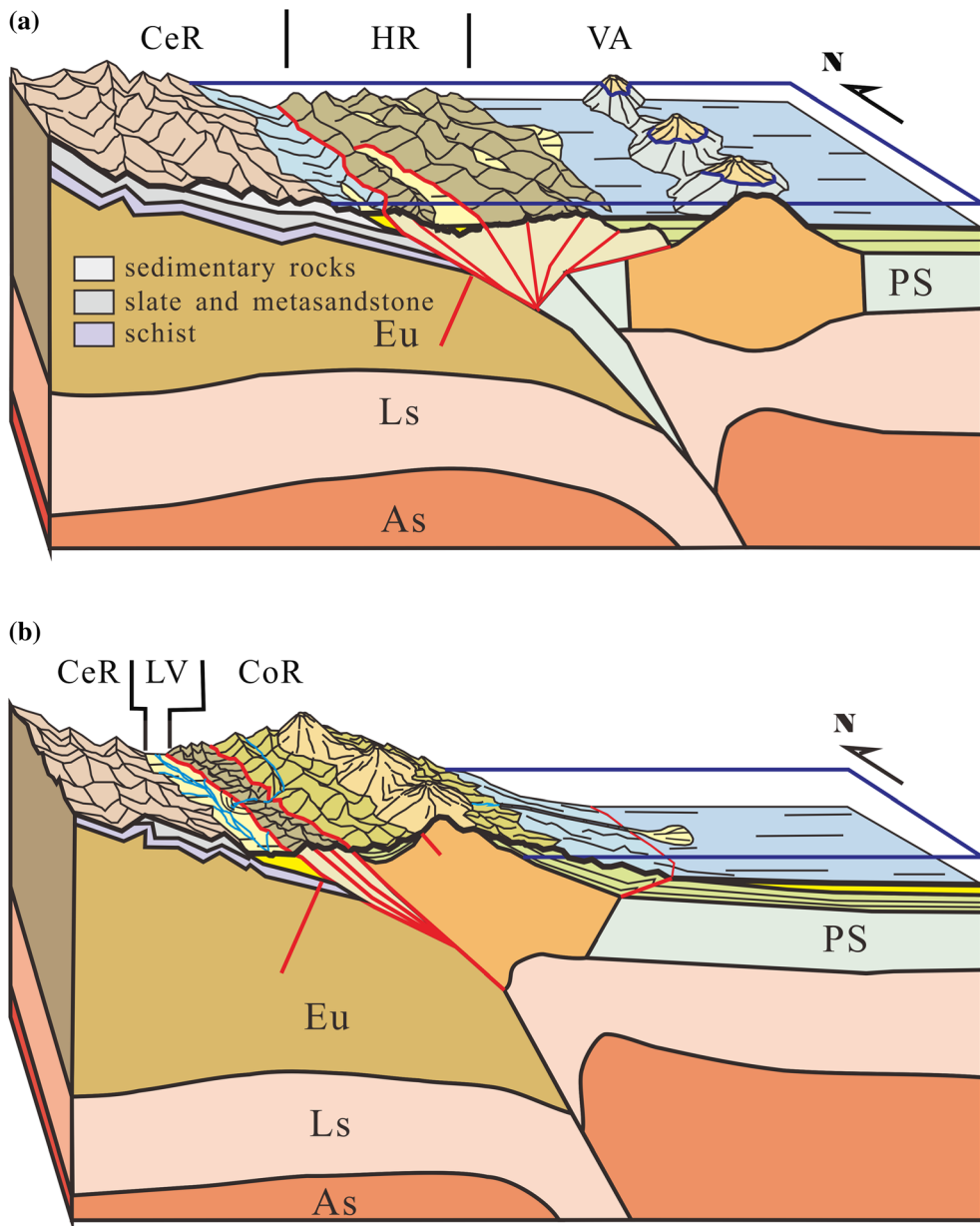


Figure 2

A block diagram of tectonic framework of the SE Taiwan Offshore (no scale; Chen 2009 with publisher's permission). **a** Tectonic setting near Green Island in the stage of initial arc-continent collision (about latitude 21.0–22.7° N). **b** Tectonic setting near Coastal Range in the stage of advanced arc-continent collision (about latitude 22.7–23.5° N). *As* asthenosphere, *CeR* central range, *CoR* coastal range, *Eu* Eurasian plate, *HR* Huatung ridge, *Ls* lithosphere (upper mantle), *LV* longitudinal valley, *PS*: Philippine sea plate, *VA* North Luzon Arc (Green and Lanyu islands)

(Kuo et al. 2017). Figure 3 shows that the Antung hot spring is situated at the hanging wall along the Yongfeng Fault and the Longitudinal Valley Fault, both of which are thrust faults. Prior to large

earthquakes, rock dilatancy is likely to take place at the hanging wall along a thrust fault (Doglionia et al. 2011, 2013).

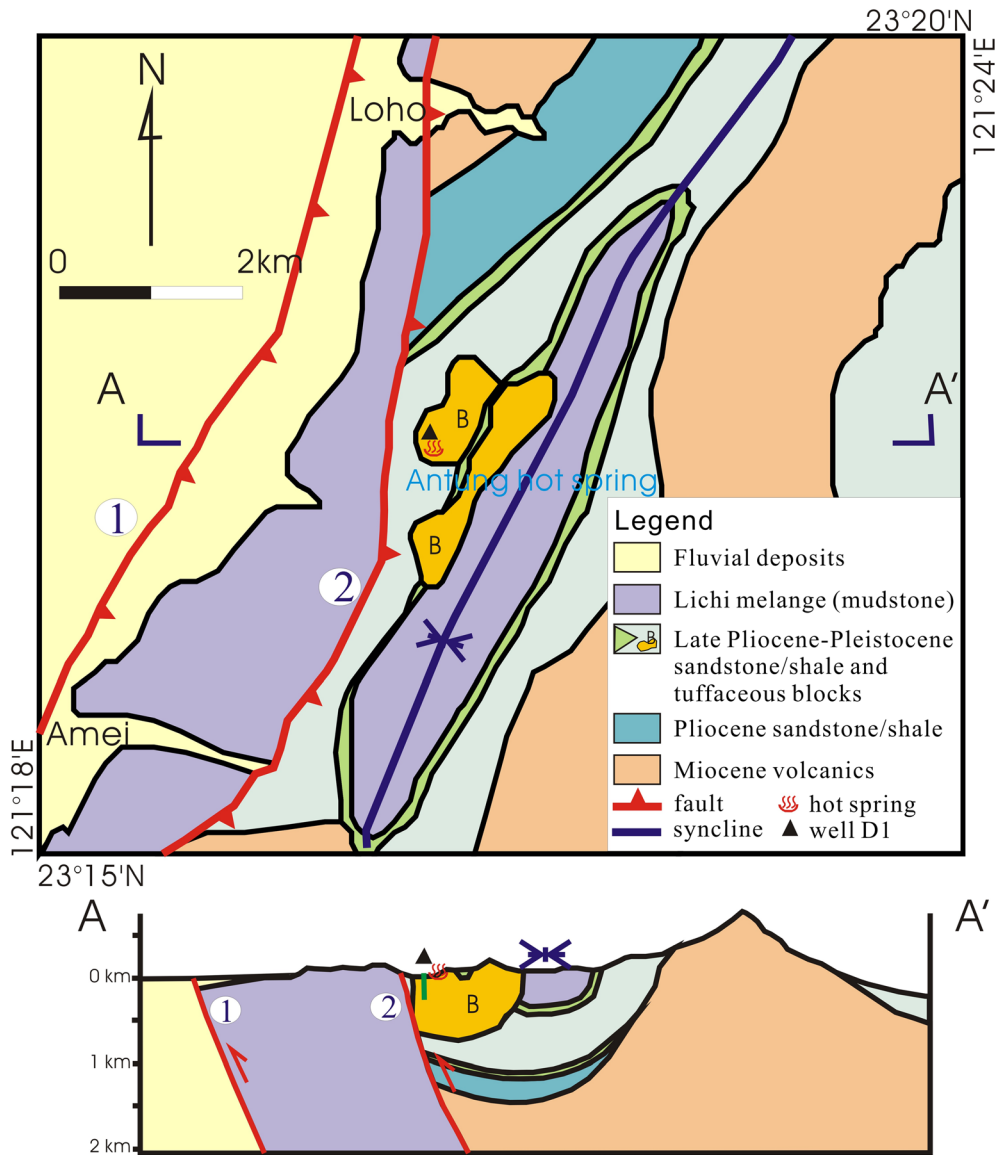


Figure 3

Geological map and cross section near the radon-monitoring well D1 in the area of Antung hot spring. (B: tuffaceous andesitic blocks; filled black triangle: radon-monitoring well D1; ①: Chihshang, or, Longitudinal Valley Fault, ②: Yongfeng Fault)

## 2.2. Seismic Data

Seismic data (geographical coordinate of epicenter and depth) were taken from earthquake catalogues of Central Weather Bureau, Taiwan. Focal mechanisms and  $M_w$  (moment magnitude scale) were from the Global CMT catalog search. Two groups of earthquakes were selected for this study. For the first group, we selected all the mainshocks ( $M_w > 6.0$ )

that occurred near the Antung hot spring between December 10, 2003 and February 21, 2018. The 2003  $M_w$  6.8 Chengkung, 2006  $M_w$  6.1 Taitung, 2013  $M_w$  6.3 Rueisuei, and 2015  $M_w$  6.2 Green Island earthquakes are the search results from the Global CMT catalog. For the second group, we selected all the mainshocks ( $M_w > 5.0$ ) that occurred between December 10, 2003 and February 21, 2018 with

epicenters located on the Longitudinal Valley fault. The 2006  $M_w$  5.9 Taitung, 2008  $M_w$  5.4 Antung, 2011  $M_w$  5.0 Chimei, and 2018  $M_w$  5.1 Changbin earthquakes are the search results from the Global CMT catalog. The focal mechanisms of the above seven events are shown in Fig. 1. Only Event 2 (April 1, 2006) and Event R (October 31, 2013) are strike-slip-faulting. All the other events are thrust-faulting.

### 2.3. Radon-Monitoring Methods

Discrete samples of groundwater water were pumped and collected from the radon-monitoring well D1 located at the Antung hot spring twice per week for analysis of radon content. The production interval of the well ranges from 167 to 187 m below ground surface. Every sampling started with flushing the stagnant water in the monitoring well and in the screen zone. An insufficiently pumped volume represents a major source of error. A minimum of three well-bored volumes were purged before taking samples for radon measurements. To achieve the above criterion, a minimum of 50 min purging-time was required with a pumping rate at around 200 L/min. Water samples were collected in a 40 mL glass vial with a TEFLON-lined cap.

It is important to ensure the radon not to escape during the sampling procedure and the sample transportation and preparation. After collecting a sample, the sample vial was inverted to check for air bubbles. If any bubbles were present in the vial, the sample water was discarded and sampling was repeated. The date and time of sample collection were recorded. The samples were stored and transported in a cooler. Counting radioactivity was done within 4 days.

The liquid scintillation method was adopted to determine the activity concentration of radon in groundwater (Noguchi 1964). Radon was partitioned selectively into a white mineral-oil based scintillation cocktail (Perkin Elmer) immiscible with the water samples, and then assayed with a liquid scintillation counter (LSC). The results were corrected for the amount of radon decay between sampling and assay.

A calibration factor for the LSC measurements of  $7.1 \pm 0.1$  cpm/pCi was calculated using an aqueous Ra-226 calibration solution, which is in secular

equilibrium with Rn-222 progeny. For a count time of 50 min and background less than 6 cpm, a detection limit below 18 pCi/L was achieved using the sample volume of 15-mL.

### 3. Results and Discussion

As shown in Fig. 4a–f, radon concentration of well D1 at Antung decreased from background levels of  $29.1 \pm 1.6$ ,  $28.2 \pm 2.1$ ,  $25.9 \pm 2.1$ ,  $27.8 \pm 0.9$ ,  $28.2 \pm 0.8$ , and  $26.6 \pm 1.2$  Bq/dm<sup>3</sup> ( $787 \pm 42$ ,  $762 \pm 57$ ,  $700 \pm 57$ ,  $752 \pm 24$ ,  $763 \pm 21$ , and  $718 \pm 32$  pCi/L) to precursory minima of  $12.1 \pm 0.3$ ,  $13.7 \pm 0.3$ ,  $17.8 \pm 1.6$ ,  $16.5 \pm 0.7$ ,  $19.8 \pm 1.0$ , and  $18.5 \pm 0.6$  Bq/dm<sup>3</sup> ( $326 \pm 9$ ,  $371 \pm 9$ ,  $480 \pm 43$ ,  $447 \pm 18$ ,  $535 \pm 28$ , and  $500 \pm 17$  pCi/L), respectively, prior to the 2003  $M_w$  6.8 Chengkung, 2006  $M_w$  6.1 and  $M_w$  5.9 Taitung, 2008  $M_w$  5.4 Antung, 2011  $M_w$  5.0 Chimei, 2015  $M_w$  6.2 Green Island, and 2018  $M_w$  5.1 Changbin earthquakes. The 2006  $M_w$  6.1 Taitung earthquake that occurred on April 1, 2006 triggered the 2006  $M_w$  5.9 Taitung earthquake that occurred on April 15, 2006 (Wu et al. 2006). All the above recurrent groundwater radon anomalies can be characterized into three stages and can be explained based on the mechanism of in situ radon volatilization (Kuo et al. 2006b). During stage 1, the radon concentration in groundwater is fairly stable; there is an accumulation of tectonic strain and a slow, steady increase of regional stress. Well D1 is completed in a small low-porosity brittle aquifer in undrained conditions. When the regional tectonic stress continues to increase, in undrained conditions, aquifer rocks could dilate at a rate faster than the rate at which groundwater could recharge into the newly created rock cracks (Nur 1972; Scholz et al. 1973). During stage 2, gas saturation and two phases (vapor and liquid) develop in the aquifer. The radon in groundwater volatilizes into the gas phase and the radon concentration in groundwater decreases (Kuo et al. 2006b). At the point of minimum radon concentration, the water saturation in cracks begins to increase again and stage 3 starts. During stage 3, the radon concentration in groundwater increases and recovers to the previous background level before the main shock.

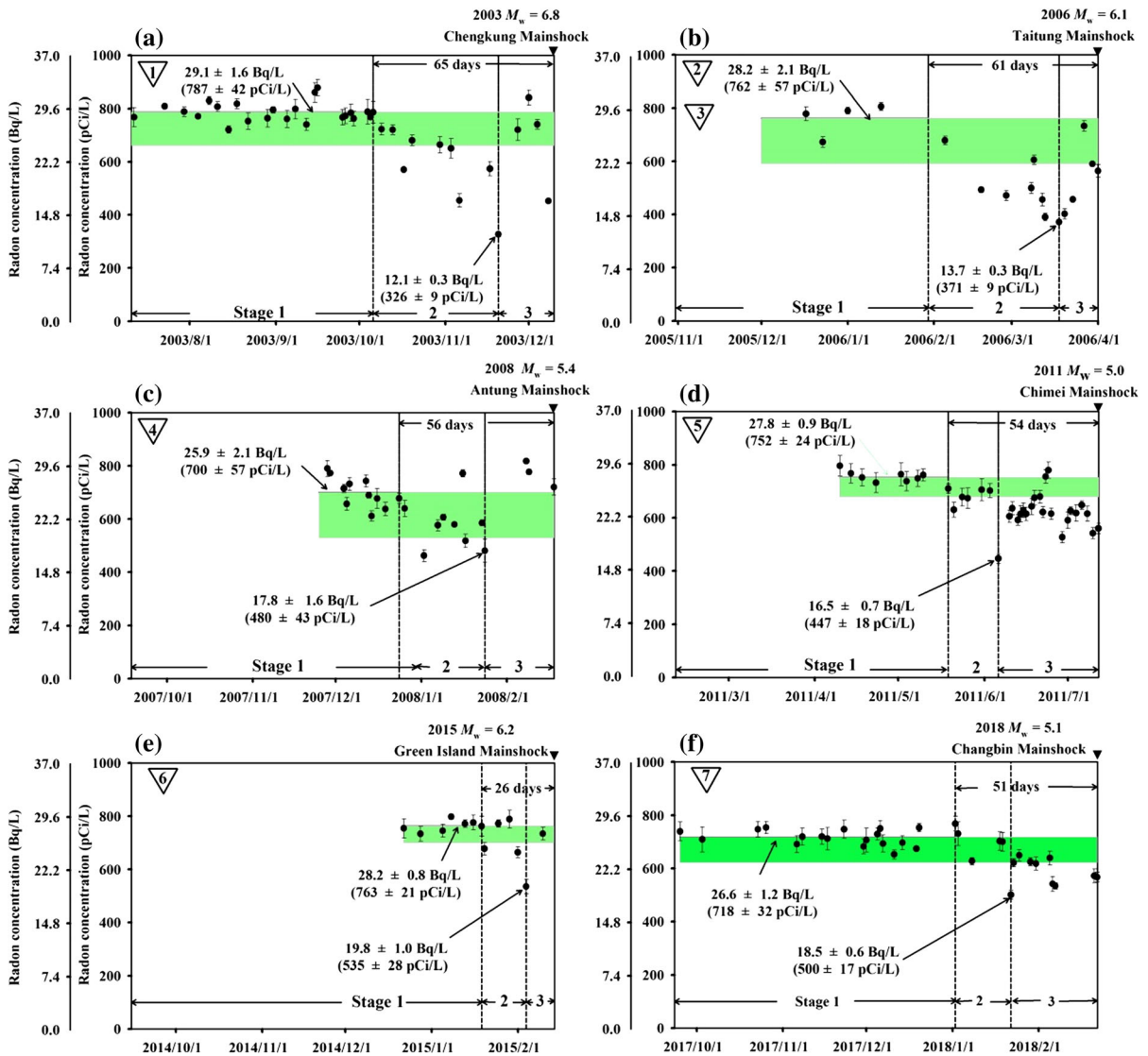


Figure 4

Radon concentration data at Antung well D1 prior to **a** 2003 Chengkung, **b** 2006 April 1 and April 15 Taitung, **c** 2008 Antung, **d** 2011 Chimei, **e** 2015 Green Island, and **f** 2018 Changbin earthquakes. Green rectangles show radon concentration between the mean radon concentration and three standard deviations below the mean. Stages 1, 2, and 3 are defined in text. Numbers in inverted triangles correspond to earthquake event in Fig. 1

An anomaly is defined as a significant deviation from the mean value, or, three standard deviations below the mean value. The mean value is calculated from the data points observed during stage 1 as shown in Fig. 4. The number of data points used to calculate the mean value are 23, 4, 11, 9, 7, and 9 for radon anomalies observed prior to 2003 Chengkung (Fig. 4a), 2006 April 1 and April 15 Taitung

(Fig. 4b), 2008 Antung (Fig. 4c), 2011 Chimei (Fig. 4d), 2015 Green Island (Fig. 4e), and 2018 Changbin (Fig. 4f) earthquakes, respectively. The rule to define stage 1, 2, and 3 is based on the trend regarding the temporal behavior of radon concentration. During stage 1, radon concentration is fairly stable. During stage 2, radon concentration decreases. During stage 3, radon concentration increases.

Due to the high background noise of radon time series (Finkelstein et al. 1998, 2006), environmental records such as atmospheric temperature, barometric pressure, and rainfall must be examined to check whether the radon anomaly could be caused by these environmental factors. A method was developed for the identification of anomalous radon concentrations due to geodynamic processes (Finkelstein et al. 1998, 2006). Radon decreased from background levels of 29.1 and 28.2 Bq/dm<sup>3</sup> to minima of 12.1 and 13.7 Bq/dm<sup>3</sup> prior to the 2003  $M_w$  6.8 Chengkung and 2006  $M_w$  6.1 Taitung earthquakes, respectively (Fig. 4a, b). There was also no heavy rainfall responsible for the radon anomaly. Besides, the atmospheric temperature, barometric pressure, and rainfall are periodic in season. It is difficult to attribute the above two large radon decreases to these environmental factors (Kuo et al. 2017).

Radon volatilization mechanism can be tested by monitoring other dissolved gases in groundwater to see whether there are simultaneous anomalous declines in groundwater radon and other dissolved gases precursory to large earthquakes. The composition of major dissolved gases at Antung well D1 consists of 62.8% of nitrogen and 36.7% of methane by volume. Simultaneous anomalous declines in groundwater radon and methane were recorded precursory to the 2008 Antung  $M_w$  5.4 earthquake (Kuo et al. 2010); thereby validating the mechanism of in situ radon volatilization.

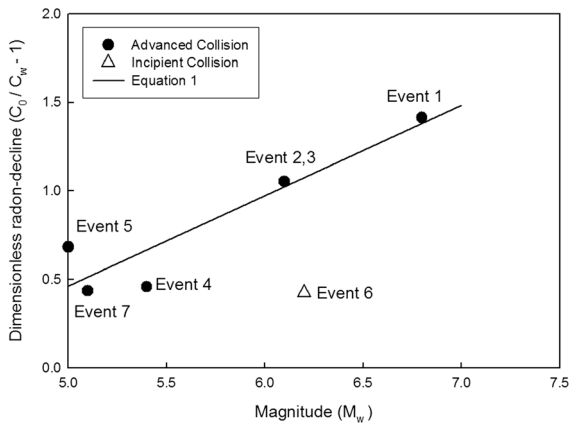


Figure 5

Dimensionless radon decline observed at well D1 as a function of earthquake magnitude ( $M_w$ ). Event 3 was triggered by Event 2

As shown in Fig. 5, Event 1, 3, 4, 5, and 7 are all thrust-type earthquakes occurring on the Longitudinal Valley Fault in advanced arc-continental collision zone. Using the radon minima precursory to the above events, the observed dimensionless radon-decline, or,  $\left(\frac{C_0}{C_w} - 1\right)$  is correlated with earthquake magnitude as follows (Kuo 2014).

$$\left(\frac{C_0}{C_w} - 1\right) = 0.5118M_w - 2.0981, \quad (1)$$

where  $C_0$  is initial radon concentration in groundwater precursory to each radon anomaly, Bq/dm<sup>3</sup> (or, pCi/L);  $C_w$  is the radon minimum in groundwater observed in well D1 during an anomalous decline, Bq/dm<sup>3</sup> (or, pCi/L);  $M_w$  is the earthquake magnitude. For earthquakes occurring on a given fault (Longitudinal Valley fault), the observed radon minima can be correlated with earthquake magnitude and crust strain. The observed precursory minimum in radon concentration decreases as the earthquake magnitude increases. Equation 1 can be quite useful locally in the southern segment of longitudinal valley for predicting earthquake magnitude occurring on the Longitudinal Valley Fault from the radon minimum observed in well D1 during an anomalous decline.

The precursor time for a radon anomaly is defined as the time interval between the moment when the concentration of groundwater radon starts to decline and the time of occurrence of the earthquake. As shown in Fig. 4a–f, the precursor times for radon anomalies precursory to Event 1, 3, 4, 5, and 7 were 65, 61, 56, 54, and 51 days, respectively. Using the precursor times precursory to the above events, the observed precursor time of radon anomaly is correlated with earthquake magnitude as follows (also shown in Fig. 6):

$$\log_{10} T = 0.0530M_w + 1.4561, \quad (2)$$

where  $T$  is the precursor time of a radon anomaly, day;  $M_w$  is the earthquake magnitude. Equations (1) and (2) are helpful for early warning of local large earthquakes from the radon minimum observed in well D1 in southeastern Taiwan. The regressed lines shown in Figs. 5 and 6 provide quantitative means to forecast both magnitude and precursory time within an approximate range for local large earthquakes occurring on the Longitudinal Valley Fault.

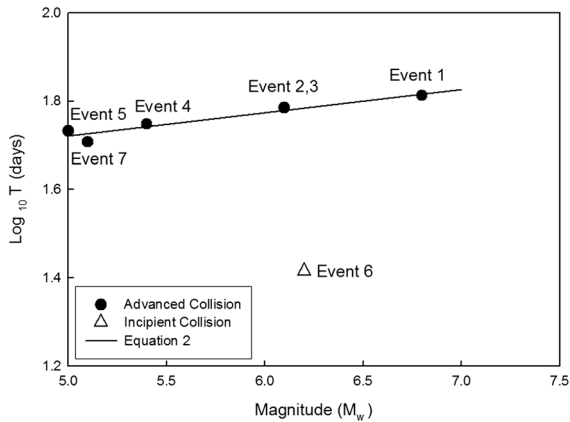


Figure 6

Precursor time of radon anomaly observed at well D1 as a function of earthquake magnitude ( $M_w$ ). Event 3 was triggered by Event 2

On February 13, 2015, an earthquake of magnitude  $M_w$  6.2 (Event 6) occurred near Green Island in southeastern Taiwan. Well D1 and the epicenter of Event 6 are located in two dissimilar tectonic settings. Well D1 is located in the tectonic setting known as Coastal Range, which represents an advanced arc-continent collision. The epicenter of Event 6 is located in the tectonic setting of an initial arc-continent collision. The observed radon anomaly prior to the above Green Island quake (Event 6) is shown in Fig. 4f. Notice that the precursory time (26 days) observed prior to Event 6 is significantly smaller than those observed prior to Event 1, 3, 4, 5, and 7 (65, 61, 56, 54, and 51 days). The open triangle shown in Figs. 5 and 6 represents Event 6 (the 2015  $M_w$  6.2 Green Island earthquake). The solid circles shown in Figs. 5 and 6 (Event 1, 3, 4, 5, and 7) can be correlated with a regressed line. Comparing the open triangle with the regressed line shown in Fig. 5, the observed radon decline prior to Event 6 is considerably smaller than those observed prior to Event 1, 3, 4, 5, and 7. Figure 6 also shows that the observed precursory time prior to Event 6 is significantly smaller than those observed prior to Event 1, 3, 4, 5, and 7. When the epicenter and radon-monitoring station are located in two dissimilar tectonic settings, both the observed radon decline and precursory time decrease because it takes additional time lag and attenuation for the stress transfer from one tectonic setting to the other. Faults also play important roles in this stress transfer lag and attenuation of the signal.

Figures 5 and 6 also imply that the correlations between radon decline, precursory time and earthquake magnitude are characteristics of the causative fault.

Between July 2003 and August 2018, eight main earthquakes occurred near Antung well D1 (Fig. 1). Anomalous decreases in the concentration of groundwater radon were observed prior to the 2003  $M_w$  6.8 Chengkung, 2006  $M_w$  6.1 and  $M_w$  5.9 Taitung, 2008  $M_w$  5.4 Antung, 2011  $M_w$  5.0 Chimei, 2015  $M_w$  6.2 Green Island, and 2018  $M_w$  5.1 Changbin earthquakes. No anomalous decline in the concentration of groundwater radon was detected at well D1 prior to the 2013 Ruesuei  $M_w$  6.3 earthquake (Kuo et al. 2017). Thus, seven successful correlations and one “omission of target”: generally speaking, these are good statistics.

#### 4. Conclusions

The significance of our research can be summarized as follows.

1. A small low-porosity fractured aquifer in undrained conditions near an active fault (e.g., Antung well D1) is a suitable geological site to detect precursory declines in groundwater radon prior to local large earthquakes in the subduction zone. Recurrent groundwater radon anomalous declines were observed at Antung well D1 prior to seven of eight main earthquakes that occurred between 2003 and 2018 ( $M_w$  range 5.0–6.8). Prior to our study, the geological conditions necessary to recurrently record radon anomalies were unknown. This paper outlines the geological requisites to site a radon observation well for earthquake forecasting.
2. The correlations between radon decline, precursory time and earthquake magnitude are characteristics of the causative fault. For earthquakes occurring on the Longitudinal Valley Fault in eastern Taiwan, the observed radon decline increases as the earthquake magnitude increases. The observed precursory time also increases as the earthquake magnitude increases. The above

correlations are useful for early warning local large earthquakes.

3. This paper investigates the differences between the radon signatures precursory to quakes in areas representing different stages of on-going plate collision in Taiwan. Given radon-monitoring well D1 located in advanced arc-continental collision zone, the radon decline and precursory time observed prior to the earthquakes occurring in initial arc-continent collision zone are smaller than those observed prior to the earthquakes occurring on the plate boundary in advanced arc-continental collision zone.
4. Via a basic observation of groundwater radon at Antung well D1, all large thrust-type earthquakes in southeastern Taiwan can be warned months in advance. We believe that it can have significant merit on a local or regional basis and most importantly, it can perhaps be applied to other areas of the world with similar tectonic settings and physical–chemical relationships. All global hazardous events in the subduction zone, such as 2004 Sumatra, 2011 Tohoku, 2018 Sulawesi and Alaska earthquakes, occurred with no warning. This paper presents the mechanism and practical applications of groundwater radon volatilization useful for forecasting future megathrust earthquakes in the subduction zone.

#### Acknowledgements

The authors are grateful to support of Industrial Technology Research Institute (Grant No. 550003318) and Mr. C. Lin for field assistance at the Antung hot spring.

**Publisher's Note** Springer Nature remains neutral with regard to jurisdictional claims in published maps and institutional affiliations.

#### REFERENCES

- Baykara, O., & Dođru, M. (2006). Measurements of radon and uranium concentration in water and soil samples from East Anatolian Active Fault Systems (Turkey). *Radiation Measurements*, *41*, 362–367.
- Brace, W. F., Paulding, B. W., Jr., & Scholz, C. H. (1966). Dilatancy in the fracture of crystalline rocks. *Journal of Geophysical Research*, *71*, 3939–3953. <https://doi.org/10.1029/JZ071i016p03939>.
- Chen, W. S. (2009). Tectonostratigraphic framework and age of the volcanic-arc and collision basins in the Coastal Range, eastern Taiwan. *Western Pacific Earth Sciences*, *9*, 67–98.
- Chen, W. S., & Wang, Y. (1996). *Geology of the Coastal Range, eastern Taiwan*. Geology of Taiwan 7. Central Geological Survey, Taiwan.
- Doglionia, C., Barbab, S., Carminatia, E., & Riguzzib, F. (2011). Role of the brittle–ductile transition on fault activation. *Physics of the Earth and Planetary Interiors*, *184*, 160–171. <https://doi.org/10.1016/j.pepi.2010.11.005>.
- Doglionia, C., Barbab, S., Carminatia, E., & Riguzzib, F. (2013). Fault on–off versus coseismic fluids reaction. *Geoscience Frontiers*, *5*, 767–780. <https://doi.org/10.1016/j.gsf.2013.08.004>.
- Erees, F. S., Aytas, S., Sac, M. M., Yener, G., & Salk, M. (2007). Radon concentrations in thermal waters related to seismic events along faults in the Denizli Basin, Western Turkey. *Radiation Measurements*, *42*, 80–86. <https://doi.org/10.1016/j.radmeas.2006.06.003>.
- Finkelstein, M., Brenner, S., Eppelbaum, L., & Ne'eman, E. (1998). Identification of anomalous radon concentration due to geodynamic processes by elimination of Rn variations caused by other factors. *Geophysical Journal International*, *133*, 407–412. <https://doi.org/10.1046/j.1365-246X.1998.00502.x>.
- Finkelstein, M., Eppelbaum, L., & Price, C. (2006). Analysis of temperature influences on the amplitude–frequency of Rn gas concentration. *Journal of Environmental Radioactivity*, *86*, 251–270. <https://doi.org/10.1016/j.jenvrad.2005.09.004>.
- Hauksson, E. (1981). Radon content of groundwater as an earthquake precursor: Evaluation of worldwide data and physical basis. *Journal of Geophysical Research*, *86*, 9397–9410. <https://doi.org/10.1029/JB086iB10p09397>.
- Hsu, T. L. (1962). Recent faulting in the Longitudinal Valley of eastern Taiwan. *Memoir of the Geological Society of China*, *1*, 95–102.
- Huang, C. Y., Yuan, P. B., & Tsao, S. J. (2006). Temporal and spatial records of active arc-continent collision in Taiwan: A synthesis. *Geological Society of America Bulletin*, *118*, 274–288.
- Igarashi, G., Saeki, S., Takahata, N., Sumikawa, K., Tasaka, S., Sasaki, Y., et al. (1995). Ground-water radon anomaly before the Kobe earthquake in Japan. *Science*, *269*, 60–61. <https://doi.org/10.1126/science.269.5220.60>.
- Kuo, T. (2014). Correlating precursory declines in groundwater radon with earthquake magnitude. *Groundwater*, *52*, 217–224. <https://doi.org/10.1111/gwat.12049>.
- Kuo, T., Cheng, W., Lin, C., Fan, K., Chang, G., & Yang, T. (2010). Simultaneous declines in radon and methane precursory to 2008 MW 5.0 Antung earthquake: Corroboration of in situ volatilization. *Natural Hazards*, *54*, 367–372.
- Kuo, T., Fan, K., Kuochen, H., & Chen, W. (2006a). A mechanism for anomalous decline in radon precursory to an earthquake. *Groundwater*, *44*, 642–647. <https://doi.org/10.1111/j.1745-6584.2006.00219.x>.
- Kuo, T., Fan, K., Kuochen, H., Han, Y., Chu, H., & Lee, Y. (2006b). Anomalous decrease in groundwater radon before the Taiwan M6.8 Chengkung earthquake. *Journal of Environmental*

- Radioactivity*, 88, 101–106. <https://doi.org/10.1016/j.jenvrad.2006.01.005>.
- Kuo, T., Kuochen, H., Ho, C., & Chen, W. (2017). A stress condition in aquifer rock for detecting anomalous radon decline precursory to an earthquake. *Pure and Applied Geophysics*, 174, 1291–1301. <https://doi.org/10.1007/s00024-016-1461-2>.
- Namvaran, M., & Negarestani, A. (2013). Measuring the radon concentration and investigating the mechanism of decline prior an earthquake (Jooshan, SE of Iran). *Journal of Radioanalytical and Nuclear Chemistry*, 298, 1–8. <https://doi.org/10.1007/s10967-013-2162-7>.
- Nevinsky, I., Tsvetkova, T., & Nevinskaya, E. (2015). Measurement of radon in ground waters of the Western Caucasus for seismological application. *Journal of Environmental Radioactivity*, 149, 19–35.
- Noguchi, M. (1964). New method of radon activity measurement with liquid scintillator. *Radioisotopes*, 13, 362–367. [https://doi.org/10.3769/radioisotopes.13.5\\_362](https://doi.org/10.3769/radioisotopes.13.5_362).
- Noguchi, M., & Wakita, H. (1977). A method for continuous measurement of radon in groundwater for earthquake prediction. *Journal of Geophysical Research*, 82, 1353–1357. <https://doi.org/10.1029/JB082i008p01353>.
- Nur, A. (1972). Dilatancy, pore fluids, and premonitory variations of ts/tp travel times. *Bulletin of the Seismological Society of America*, 62, 1217–1222.
- Papastefanou, C. (2002). An overview of instrumentation for measuring radon in soil gas and groundwaters. *Journal of Environmental Radioactivity*, 63, 271–283. [https://doi.org/10.1016/S0265-931X\(02\)00034-6](https://doi.org/10.1016/S0265-931X(02)00034-6).
- Scholz, C. H., Sykes, L. R., & Aggarwal, Y. P. (1973). Earthquake prediction: A physical basis. *Science*, 181, 803–810. <https://doi.org/10.1126/science.181.4102.803>.
- Shapiro, M. H., Melvin, J. D., & Tombrello, T. A. (1980). Automated radon monitoring at a hard-rock site in the southern California transverse ranges. *Journal of Geophysical Research*, 85, 3058–3064. <https://doi.org/10.1029/JB085iB06p03058>.
- Skelton, A., Andrén, M., Kristmannsdóttir, H., Stockmann, G., Mörth, C., Sveinbjörnsdóttir, Á., et al. (2014). Changes in groundwater chemistry before two consecutive earthquakes in Iceland. *Nature Geoscience*, 7, 752–756.
- Tarakçı, M., Harmanşah, C., Saç, M. M., & İçhedef, M. (2014). Investigation of the relationships between seismic activities and radon level in western Turkey. *Applied Radiation and Isotopes*, 83, 12–17. <https://doi.org/10.1016/j.apradiso.2013.10.008>.
- Wakita, H., Nakamura, Y., Notsu, K., Noguchi, M., & Asada, T. (1980). Radon anomaly: A possible precursor of the 1978 Izu-Oshima-kinkai earthquake. *Science*, 207, 882–883. <https://doi.org/10.1126/science.207.4433.882>.
- Wu, Y. M., Chen, Y. G., Chang, C. H., Chung, L. H., Teng, T. L., Wu, F. T., et al. (2006). Seismogenic structure in a tectonic suture zone: With new constraints from 2006 Mw6.1 Taitung earthquake. *Geophysical Research Letters*, 33, L22305.
- Yalim, H. A., Sandıkcıoğlu, A., Ünala, R., & Orhunb, Ö. (2007). Measurements of radon concentrations in well waters near the Akşehir fault zone in Afyonkarahisar, Turkey. *Radiation Measurements*, 42, 505–508. <https://doi.org/10.1016/j.radmeas.2006.12.013>.
- Zmazeka, B., Todorovskia, L., Živčiča, M., Džeroskia, S., Vau-potiča, J., & Kobala, I. (2006). Radon in a thermal spring: Identification of anomalies related to seismic activity. *Applied Radiation and Isotopes*, 64, 725–734. <https://doi.org/10.1016/j.apradiso.2005.12.016>.

(Received May 2, 2019, revised October 17, 2019, accepted December 5, 2019)